IEEE Journal of Microwaves

Received 10 March 2022; revised 27 April 2022 and 18 June 2022; accepted 14 July 2022. Date of publication 11 August 2022; date of current version 7 October 2022.

Digital Object Identifier 10.1109/JMW.2022.3192114

A Compact Dual-Band Differential Negative Group Delay Circuit With Wideband Common Mode Suppression

ZHONGBAO WANG (Member, IEEE), SHIPENG ZHAO, HONGMEI LIU, AND SHAOJUN FANG

(Regular Paper)

School of Information Science and Technology, Dalian Maritime University, Dalian 116026, China

CORRESPONDING AUTHOR: Zhongbao Wang (e-mail: wangzb@dlmu.edu.cn).

This work was supported in part by the National Natural Science Foundation of China under Grant 61871417, in part by the LiaoNing Revitalization Talents Program under Grant XLYC2007024, in part by the Natural Science Foundation of Liaoning Province under Grant 2020-MS-127, and in part by the Fundamental Research Funds for the Central Universities under Grant 3132022243.

ABSTRACT A compact dual-band differential negative group delay (DNGD) circuit with wideband common mode suppression is proposed. Two small 180° phase shift swap structures of double-sided parallel striplines (DSPS) are adopted to realize intrinsic wideband common-mode suppression. The dual-band DNGD characteristic is achieved by the DSPS coupled asymmetrically with two different-length open-circuited resonators. The DNGD times and center frequencies of the lower and upper bands can be tuned independently. To verify the proposed DNGD circuit topology, a prototype is designed, fabricated, and measured. From the measured results, DNGD times are −1.60 ns and −1.43 ns at the center frequencies of 1.227 GHz and 1.575 GHz, respectively. The differential insertion loss is lower than 3.55 dB, the differential return loss is larger than 13.3 dB and the common-mode suppression is over 30.8 dB in both DNGD bands.

INDEX TERMS Common-mode suppression, dual-band, DSPS, negative group delay.

I. INTRODUCTION

In recent years, with the rapid development of high-speed electronic systems, balanced/differential circuits have been utilized widely due to their excellent performance in terms of the immunity against environmental noises and electromagnetic interferences, compared with the single-end counterparts [1]. To combine the balanced active circuits and differentially driven antennas to build up fully balanced transceivers, various balanced passive components have been proposed, such as balanced filter [2], balanced coupler [3], and balanced power divider [4].

The group delay (GD) is a key parameter in microwave circuits and systems [5]. In the pseudo-range measurement of the global navigation satellite systems (GNSS), the distortion of the group delay will cause the increase of the system measurement error [6]. For these reasons, the GD equalization technique based on the negative group delay (NGD) has been proposed [7]–[10]. In [11], a reconfigurable negative group delay circuit (NGDC) based on the branch-line coupler was proposed. By simply adjusting the capacitance values, both the transmission gain/loss and group delay values of the NGDC can be independently adjusted as desired. But it needs to insert two amplifiers in the transmission paths to compensate for the transmission loss. Various approaches for the implementation of RF passive devices integrated with NGD characteristics have been presented [12]–[17]. In [12], a novel and generalized planar coupler with four independent arbitrary terminated resistances, unequal power division, and wideband positive and negative group delays was proposed. In [13], a full-passband linear-phase bandpass filter was presented and the NGDC was utilized to suppress the salient group delay at the edge of the passband of the traditional bandpass filter for achieving the full-passband linear-phase characteristic. Several kinds of RF power dividers integrated with NGD characteristics can be achieved using the coupling matrix approach [14]–[17]. All mentioned RF passive devices focus on improving the phase characteristics of their devices by integrating NGD characteristics. However, these

RF passive counterparts are single-ended and unsuitable for use in balanced systems to reduce interference from common-mode noise.

Furthermore, with the rapid development of various wireless systems for multiple-access and multifunctional applications, several dual-band NGDCs have been designed in [18]–[21] to satisfy the GD compensation for multiband devices. In [18], [19], the frequency ratio of the upper and lower bands is decided by the characteristic impedance of the transmission lines. However, the upper and lower NGD operation frequencies f_1 and f_2 rely on the frequency $f_0 = (f_1 + f_2)/2$. To independently control the center frequency and NGD time, a dual-band NGDC with the defected structures was proposed [20]. The center frequency can be changed by the defected structures and the NGD time of each band can be tuned by the loaded resistors. But it has to face the problem of large insertion loss (IL). In [21], a dual-band NGDC with multi-coupled lines was proposed. The disadvantage is that the circuit dimension is slightly larger. In addition, an approach to applying the NGD circuit to a multi-band system is detailed in [22], but higher-order and in-series-cascade multi-stage realizations increase the complexity of the circuit design. In order to achieve a differential circuit with common-mode noise suppression, negative group delay properties can also be implemented to improve the phase behavior of the circuit, two balanced circuits integrated with differential negative group delay (DNGD) characteristics have been presented [23], [24]. However, the common-mode suppression (CMS) is poor. To the best of our knowledge, the dual-band DNGD circuit has not been reported before. Therefore, it is necessary to design a dual-band DNGD circuit to accommodate various wireless systems for multiple-access and multifunctional applications and to achieve excellent common-mode noise suppression in balanced systems.

In this paper, a compact dual-band differential negative group delay circuit (DNGDC) with wideband common-mode suppression is proposed. The proposed DNGDC is composed of two small 180° phase shift swap structures and the double-sided parallel striplines (DSPS) coupled asymmetrically with two different-length open-circuited resonators. Excellent common-mode suppression and the DNGD characteristic can be integrated into this dual-band balanced circuit, which has a flexible design of operation frequencies (f_1 and f_2) and DNGD times. The analysis and results of the proposed dual-band DNGDC are given and discussed. And it can be applied in dual-band balanced GPS L1 band and L2 band system to shorten the delay lines and suppress the common mode interference.

II. DESIGN OF THE PROPOSED DUAL-BAND DNGDC

The configuration of the proposed dual-band DNGDC is shown in Fig. 1. It is originally implemented with two small 180° phase shift swap structures and the asymmetrically coupling between the main transmission line and the λ/2

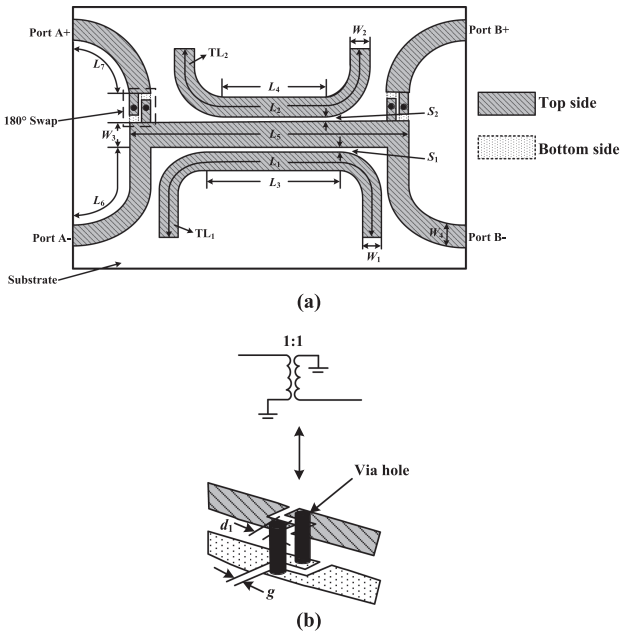

FIGURE 1. Configuration of the proposed dual-band DNGDC. (a) Top view. (b) DSPS 180° swap.

open-circuited resonators, which are realized with DSPS. The 180° phase shift swap structures deliver excellent wideband common-mode suppression properties with a compact structure. The DNGD characteristic of the proposed dual-band DNGDC is generated by the open-circuited DSPS resonators. Therefore, the DNGD value is mainly determined by the width of the open-circuited DSPS resonators (W_1 and W_2) and coupling gaps (S_1 and S_2). The DNGD operation frequencies of the proposed dual-band DNGDC (f_1 and f_2) can be independently adjusted by the length of two open-circuited DSPS resonators (L_1 and L_2).

Fig. 2 gives the effects of the open-circuited DSPS resonator TL1 on the performances of the proposed DNGDC. When the length of the TL1 (L_1) is increased from 37.18 to 45.18 mm, the center frequency of the lower DNGD band varies inversely to L_1. The change of the DNGD value and differential insertion loss ($|S_{ddBA}|$) at the center frequency of the lower DNGD band is negligible. Meanwhile, during the width of the TL1 (W_1) is increased from 2 to 6 mm, the center frequency of the lower DNGD band is also increased. On the contrary, the DNGD absolute value and differential insertion loss at the center frequency of the lower DNGD band are decreased with the increase of W_1. Furthermore, the performances in the upper DNGD band are less sensitive to the open-circuited DSPS resonator TL1. On the contrary, the open-circuited DSPS resonator TL2 has a negligible effect on the lower DNGD band and a similar effect on the upper DNGD band, as shown in Fig. 3. Therefore, by tuning (L_1, W_1) and (L_2, W_2), the independent adjustment of the lower and upper DNGD bands can be achieved.

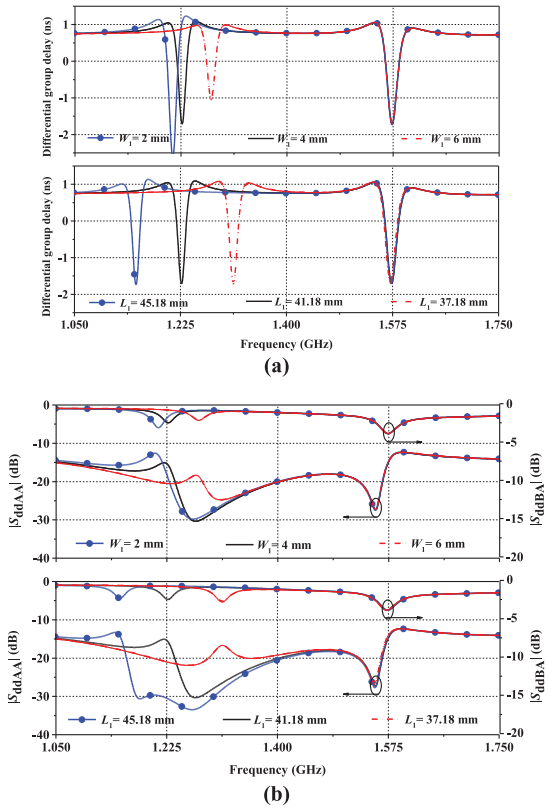

FIGURE 2. Effect of W_1 and L_1 on the performances of the proposed dual-band DNGDC. (a) GD. (b) Mixed *S*-parameters.

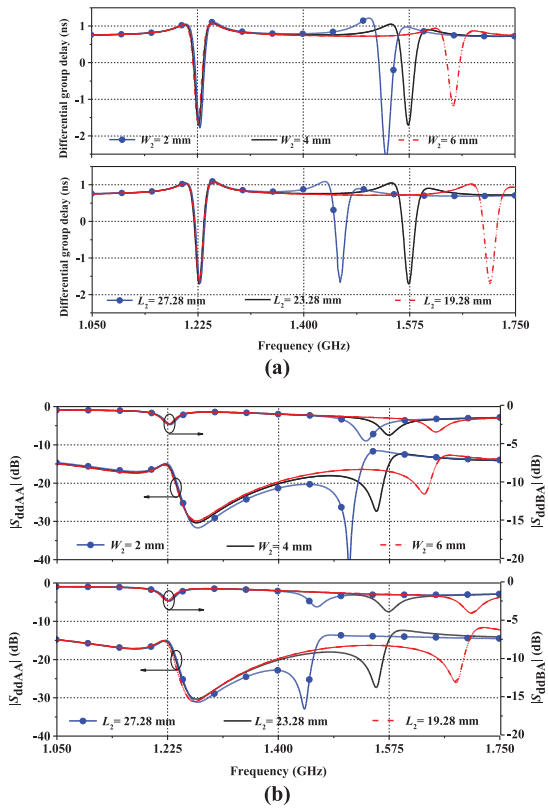

FIGURE 3. Effect of W_2 and L_2 on the performances of the proposed dual-band DNGDC. (a) GD. (b) Mixed *S*-parameters.

Fig. 4 shows the effects of the coupling length (L_3 and L_4) of two open-circuited resonators with the unchanged total length (L_1 and L_2) on the performance of the proposed DNGDC. When the coupling length L_3 is increased from 18.18 to 26.18 mm, only the differential group delay (DGD) and $|S_{ddAA}|$ in the lower DNGD band have minor changes. When the coupling length L_4 is increased from 10.12 to 18.12 mm, the DNGD absolute value and differential insertion loss at the center frequency of the upper DNGD band are increased. Fig. 5 shows the effects of the coupling gaps (S_1 and S_2) on the performance of the proposed DNGDC. During S_1 is increased from 0.13 to 0.33 mm, the DNGD absolute value at the center frequency of the lower DNGD band is decreased and the performances in the upper DNGD band are unchanged. During S_2 is increased from 0.1 to 0.3 mm, the DNGD absolute value at the center frequency of the upper DNGD band is decreased and the performances in the lower DNGD band are unchanged. The gaps of the coupling sections S_1 and S_2 have independent effects on the lower and upper bands. Therefore, when tuning S_1 and S_2, the center frequency is slightly changed, but the independent adjustment of DNGD time for both bands can be achieved.

Fig. 6 gives the effects of the main transmission line on the performance of the proposed DNGDC. When the width of the main transmission line (W_3) is increased from 3 to 7 mm, the DNGD absolute values at the center frequencies of both DNGD bands are increased but the $|S_{ddAA}|$ in the upper DNGD band becomes worse. When the length of the main transmission line (L_5) is decreased from 52.6 to 48.6 mm, the $|S_{ddAA}|$ in the upper DNGD band becomes better but the $|S_{ddAA}|$ in the lower DNGD band is degraded. Therefore, there is a trade-off in the choice of the width and length of the main transmission line.

According to the foregoing analysis, the design flow of the proposed dual-band DNGDC can be organized in the following six successive actions.

1) Determine the DNGD time and the center frequencies of the lower and upper bands (f_1 and f_2) based on the design requirements. Obtain the values of relative dielectric constant ε_r and thickness h of the substrate.
2) Adopt 180° phase shift swap structures of DSPS to realize excellent common-mode suppression.
3) Select the appropriate length (L_5) and width (W_3) of the main transmission line according to Fig. 6.
4) Choose proper widths W_1 and W_2 according to Figs. 2 and 3. Then calculate the lengths L_1 and L_2 to be about $\lambda/2$ at f_1 and f_2, respectively.
5) Adjust the coupling gaps S_1 and S_2 referring to Fig. 5 to obtain the required DNGD times.
6) Tune L_1 and L_2 according to Figs. 2 and 3 to achieve the needed frequencies f_1 and f_2.

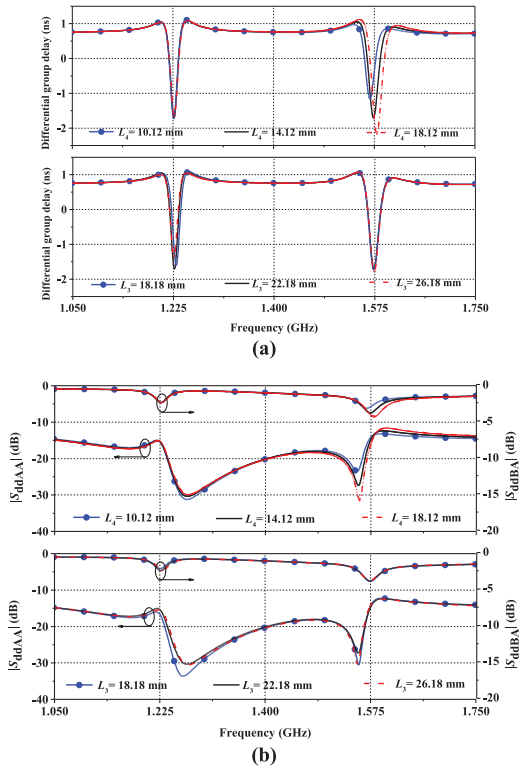

FIGURE 4. Effect of L_3 and L_4 on the performances of the proposed dual-band DNGDC. (a) GD. (b) Mixed *S*-parameters.

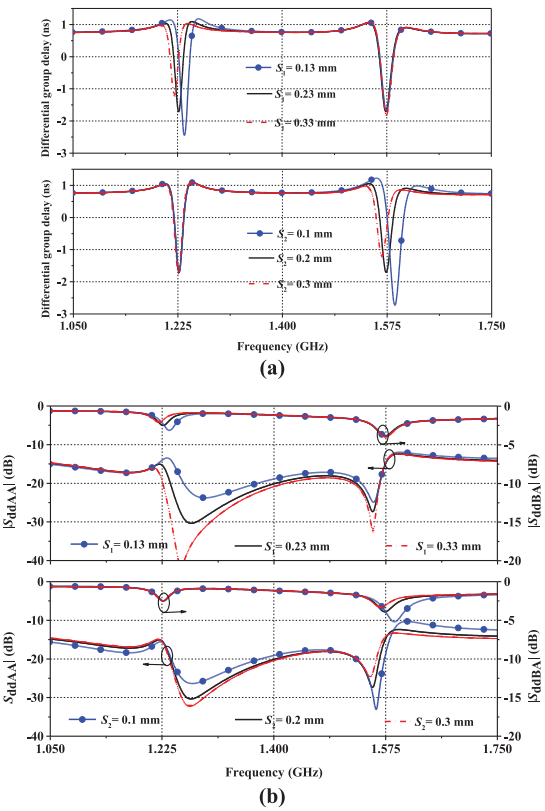

FIGURE 5. Effect of S_1 and S_2 on the performances of the proposed dual-band DNGDC. (a) GD. (b) Mixed *S*-parameters.

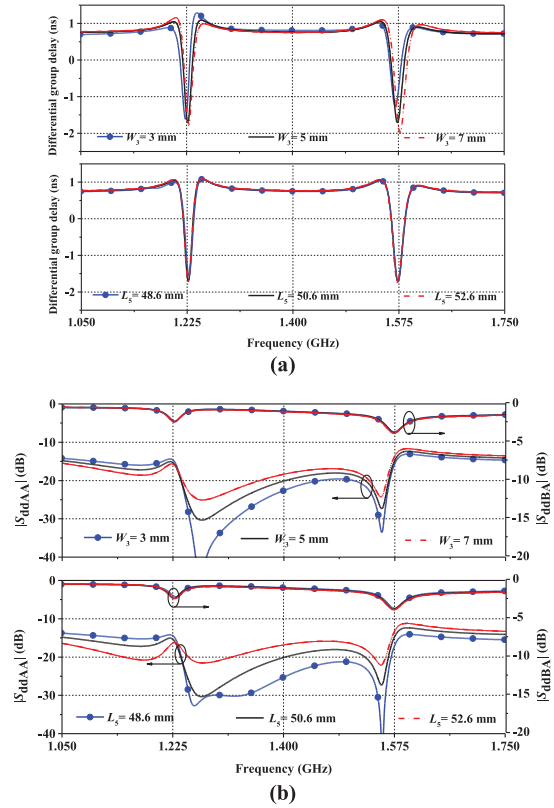

FIGURE 6. Effect of W_3 and L_5 on the performances of the proposed dual-band DNGDC. (a) GD. (b) Mixed *S*-parameters.

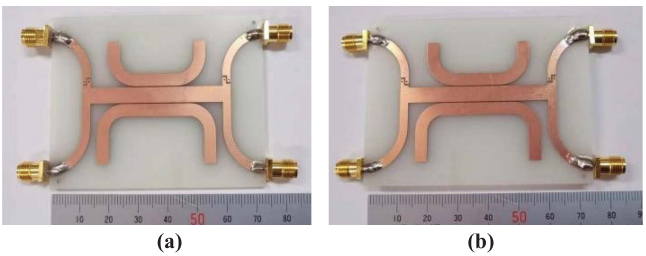

FIGURE 7. Photographs of the fabricated dual-band DNGDC. (a) Top view. (b) Bottom view.

III. IMPLEMENTATION AND PERFORMANCE

To validate the design concept of the proposed DNGDC topology, a dual-band DNGDC is designed with the center frequency of the lower band $f_1 = 1.227$ GHz and the center frequency of the upper band $f_2 = 1.575$ GHz. The prototype of the proposed DNGDC is fabricated on a 1 mm-thick substrate with a relative dielectric constant of 4.4 and loss tangent of 0.02. After optimizing by ANSYS HFSS, the physical dimensions are obtained as follows: $L_1 = 41.18$ mm, $W_1 = 4$ mm, $L_2 = 23.28$ mm, $W_2 = 4$ mm, $L_3 = 22.18$ mm, $L_4 = 14.12$ mm, $L_5 = 50.6$ mm, $W_3 = 5$ mm, $L_6 = 28$ mm, $L_7 = 22$ mm, $W_4 = 2.8$ mm, $S_1 = 0.23$ mm, and $S_2 = 0.2$ mm. Fig. 7 illustrates the photograph of the fabricated dual-band DNGDC. The circuit size of the prototype is 73 mm ×

TABLE 1. Performance Comparison

Reference	f_i (GHz)	NGD (ns)	IL (dB)	RL (dB)	NGD FBW (%)	FOM	Size ($\lambda_g \times \lambda_g$)	CMS (dB)	Flexible Design
[18]	0.667	−1.2	18.2	24.8	34.5	0.0338	0.27 × 0.13	-	No
	1.377	−1.2	18.2	24.7	16.5	0.0332			
[19]	0.496	−2.9	8.3	23.3	7.66	0.0426	0.50 × 0.19	-	No
	1.499	−3.1	10.2	25.4	3.67	0.0519			
[20]	3.500	−4.5	47.2	-	3.43	0.0023	0.64 × 0.36	-	Yes
	5.150	−4.2	38.8	-	1.94	0.0048			
[21]	2.436	−4.1	2.13	12.6	0.49	0.0381	1.47 × 1.26	-	No
	3.022	−3.8	2.86	12.4	0.43	0.0358			
[23]	1.000	−0.22	3.7	10.5	8.8	0.0126	-	18	-
[24]	1.800	−1.10	2.4	15.0	-	-	0.25 × 0.55	15	-
This work	1.227	−1.60	2.49	14.5	1.47	0.0217	0.41 × 0.30	30.8	Yes
	1.575	−1.43	3.55	13.3	1.46	0.0222			

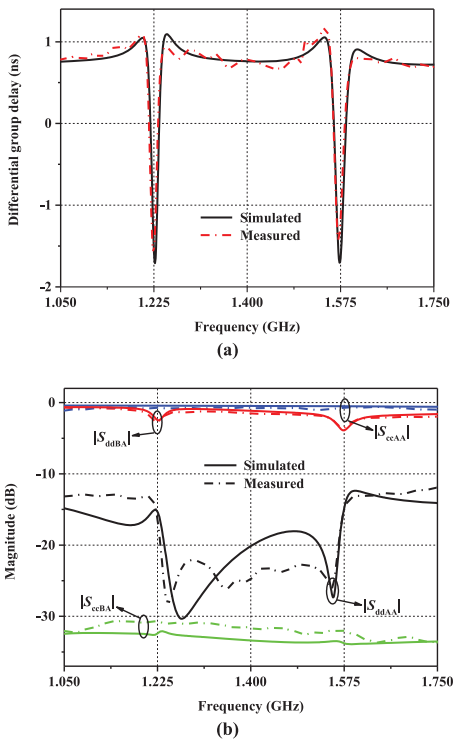

FIGURE 8. Simulated and measured results of the proposed dual-band DNGDC. (a) GD. (b) Mixed *S*-parameters.

54.1 mm (around $0.41\lambda_g \times 0.30\lambda_g$, where λ_g is the guided wavelength of 50-Ω transmission line at f_1). The fabricated dual-band DNGDC prototype is measured with an Agilent N5230A network analyzer.

Fig. 8 shows the measured results of DGD and mixed *S*-parameters, along with simulated ones for comparison. For f_1 of 1.227 GHz, the measured DGD and $|S_{ddBA}|$ are −1.60 ns and −2.49 dB, respectively. The lower DNGD bandwidth (the bandwidth for DGD less than 0 ns) is 1.47% (1.217–1.235 GHz). The differential return loss (RL) is better than 14.5 dB (i.e., $|S_{ddAA}| < -14.5$ dB) in the lower DNGD band. For the upper band, the measured DGD and $|S_{ddBA}|$ at $f_2 = 1.575$ GHz are −1.43 ns and −3.55 dB, respectively. The upper DNGD fractional bandwidth (FBW) is 1.46% from 1.562 to 1.585 GHz. The differential RL is better than 13.3 dB in the upper DNGD band. As shown in Fig. 8, the measured $|S_{ccBA}|$ is less than −30.8 dB from 1.05 to 1.75 GHz, wideband and large common-mode suppression is obtained. There are some discrepancies between the simulated and measured results, which are mainly due to inaccurate dielectric constant and loss of the used FR4 substrate in the prototype and fabrication tolerance.

The comparison of the proposed dual-band DNGDC with previous works is shown in Table I. Compared with [18]–[21], [23], [24], the proposed balanced dual-band DNGDC with outstanding CMS has a flexible design of operation frequencies (f_1 and f_2) and DNGD times. Furthermore, the proposed DNGDC has a small insertion loss, compact circuit structure, and moderate figure of merit (FOM), where the FOM is defined as

$$\mathrm{FOM} = |\mathrm{NGD}\,(f_i)| \times \mathrm{BW}_{\mathrm{NGD}} \times |S_{21}\,(f_i)| \qquad (1)$$

IV. CONCLUSION

In this paper, a compact dual-band DNGDC with wideband CMS has been presented. Two small 180° phase shift swap structures of DSPS deliver excellent common-mode rejection properties with a compact structure. The dual-band DNGD characteristic is generated by the DSPS coupled asymmetrically with open-circuited resonators. Compared to the existing NGDCs, the proposed dual-band DNGDC is integrated with excellent CMS and has the advantage of flexible design of operation frequencies and DNGD times. So it can be applied in dual-band balanced GPS L1 band and L2 band system to shorten the delay lines and suppress the common-mode interference.

REFERENCES

[1] F. Wei, Z. Y. Yang, P. Y. Qin, Y. J. Guo, B. Li, and X. W. Shi, "A balanced-to-balanced in-phase filtering power divider with high selectivity and isolation," *IEEE Trans. Microw. Theory Techn.*, vol. 67, no. 2, pp. 683–694, Feb. 2019.

[2] W. Feng, B. Pan, H. Zhu, X. Y. Zhou, W. Che, and Q. Xue, "High performance balanced bandpass filters with wideband common mode suppression," *IEEE Trans. Circuits Syst. II, Exp. Briefs*, vol. 68, no. 6, pp. 1897–1901, Jun. 2021.

[3] L. Li, L. S. Wu, J. Mao, M. Tang, and X. W. Gu, "A balanced-to-balanced rat-race coupling network based on defected slots," *IEEE Microw. Wireless Compon. Lett.*, vol. 29, no. 7, pp. 459–461, Jul. 2019.

[4] B. Xia, L. Wu, and J. Mao, "A new balanced-to-balanced power divider/combiner," *IEEE Trans. Microw. Theory Techn.*, vol. 60, no. 9, pp. 2791–2798, Sep. 2012.

[5] F. Wan et al., "0IO-shape PCB trace negative group-delay analysis," *IEEE Access*, vol. 8, pp. 97707–97717, 2020.

[6] Z. Wang, Y. Bai, Y. Meng, S. Fang, and H. Liu, "A compact negative group delay circuit topology based on asymmetric coplanar striplines and double-sided parallel striplines," *Prog. Electromagn. Res. Lett.*, vol. 98, pp. 139–144, Jul. 2021.

[7] Z. Wang, Y. Cao, T. Shao, S. Fang, and H. Liu, "A negative group delay microwave circuit based on signal interference techniques," *IEEE Microw. Wireless Compon. Lett.*, vol. 28, no. 4, pp. 290–292, Apr. 2018.

[8] T. Shao, Z. Wang, S. Fang, H. Liu, and Z. N. Chen, "A full-passband linear-phase band-pass filter equalized with negative group delay circuits," *IEEE Access*, vol. 8, pp. 43336–43343, 2020.

[9] G. Chaudhary and Y. Jeong, "A design of compact wideband negative group delay network using cross coupling," *Microw. Opt. Technol. Lett.*, vol. 56, no. 11, pp. 2495–2497, Nov. 2014.

[10] B. Ravelo, "Theory of coupled line coupler-based negative group delay microwave circuit," *IEEE Trans. Microw. Theory Techn.*, vol. 64, no. 11, pp. 3604–3611, Nov. 2016.

[11] T. Zhang, T. Yang, and P. L. Chi, "Novel reconfigurable negative group delay circuits with independent group delay and transmission loss/gain control," *IEEE Trans. Microw. Theory Techn.*, vol. 68, no. 4, pp. 1293–1303, Apr. 2020.

[12] Y. Wu, H. Wang, Z. Zhuang, Y. Liu, Q. Xue, and A. A. Kishk, "A novel arbitrary terminated unequal coupler with bandwidth-enhanced positive and negative group delay characteristics," *IEEE Trans. Microw. Theory Techn.*, vol. 66, no. 5, pp. 2170–2184, May 2018.

[13] T. Shao, Z. Wang, S. Fang, H. Liu, and Z. N. Chen, "A full-passband linear-phase band-pass filter equalized with negative group delay circuits," *IEEE Access*, vol. 8, pp. 43336–43343, 2020.

[14] G. Chaudhary and Y. Jeong, "Negative group delay phenomenon analysis in power divider: Coupling matrix approach," *IEEE Trans. Compon., Packag., Manuf. Technol.*, vol. 7, no. 9, pp. 1543–1551, Sep. 2017.

[15] G. Chaudhary and Y. Jeong, "A design of power divider with negative group delay characteristics," *IEEE Microw. Wireless Compon. Lett.*, vol. 25, no. 6, pp. 394–396, Jun. 2015.

[16] F. Wan, N. Li, B. Ravelo, and J. Ge, "O=O shape low-loss negative group delay microstrip circuit," *IEEE Trans. Circuits Syst. II, Exp. Briefs*, vol. 67, no. 10, pp. 1795–1799, Oct. 2020.

[17] J. K. Xiao, Q. F. Wang, and J. G. Ma, "A matched negative group delay circuit and its integration with an unequal power divider," *IEEE Access*, vol. 7, pp. 113578–113588, 2019.

[18] T. Shao, S. Fang, Z. Wang, and H. Liu, "A compact dual-band negative group delay microwave circuit," *Radioengineering*, vol. 27, no. 4, pp. 1070–1076, Dec. 2018.

[19] Y. Meng, Z. Wang, S. Fang, T. Shao, H. Liu, and Z. Chen, "Dual-band negative group delay microwave circuit with low signal attenuation and arbitrary frequency ratio," *IEEE Access*, vol. 8, pp. 49908–49919, 2020.

[20] G. Chaudhary, Y. Jeong, and J. Lim, "Miniaturized dual-band negative group delay circuit using dual-plane defected structures," *IEEE Microw. Wireless Compon. Lett.*, vol. 24, no. 8, pp. 521–523, Aug. 2014.

[21] X. Zhou et al., "Analytical design of dual-band negative group delay circuit with multi-coupled lines," *IEEE Access*, vol. 8, pp. 72749–72756, 2020.

[22] R. Gómez-García, J.-M. Muñoz-Ferreras, and D. Psychogiou, "Adaptive multi-band negative-group-delay microwave circuits with low reflection," *IEEE Trans. Circuits Syst. I, Reg. Papers*, vol. 68, no. 5, pp. 2196–2209, May 2021.

[23] Z. Zhu, Z. Wang, Y. Meng, S. Fang, and H. Liu, "Balanced microstrip circuit with differential negative group delay characteristics," in *Proc. Cross Strait Radio Sci. Wireless Technol. Conf.*, 2021, pp. 257–259.

[24] J. Shi, Z. Chen, and K. Xu, "Negative group delay power dividing network with balanced-to-single-ended topology," *IET Microw. Antennas Propag.*, vol. 13, no. 10, pp. 1705–1710, Aug. 2019.

ZHONGBAO WANG (Member, IEEE) received the Ph.D. degree in communication and information systems from Dalian Maritime University (DMU), Dalian, China, in 2012. He is currently a Full Professor with the School of Information Science and Technology, DMU. From 2014 to 2018, he was a Postdoctoral Fellow with the Beijing University of Posts and Telecommunications, Beijing, China. From 2019 to 2020, he was a Visiting Scholar with the Department of Electrical and Computer Engineering, National University of Singapore, Singapore. He has authored or coauthored two books and more than 90 papers in journals and conferences. His current research interests include passive RF components, patch antennas, and microwave technology using artificial intelligence. He is currently a technical reviewer of IEEE TRANSACTIONS ON MICROWAVE THEORY AND TECHNIQUES, IEEE TRANSACTIONS ON CIRCUITS AND SYSTEMS, IEEE TRANSACTIONS ON INDUSTRIAL ELECTRONICS, IEEE MICROWAVE AND WIRELESS COMPONENTS LETTERS, IEEE ANTENNAS AND WIRELESS PROPAGATION LETTERS, IEEE ACCESS, *IET Microwaves*, *Antennas and Propagation*, *Electronics Letters*, *Radioengineering*, *International Journal of RF and Microwave Computer-Aided Engineering*, and *AEU-International Journal of Electronics and Communications*. He was the recipient of the Best Doctor's Dissertation Award of Liaoning Province in 2013.

SHIPENG ZHAO received the B.Eng. degree in electronic information science and technology in 2021 from Dalian Maritime University (DMU), Dalian, China, where he is currently working toward the M.Eng. degree in information and communication engineering. His current research interests include balanced components and negative group delay.

HONGMEI LIU received the Ph.D. degree in communication and information systems from Dalian Maritime University (DMU), Dalian, China, in 2016. She is currently an Associate Professor with the School of Information Science and Technology, DMU. Her current research interests include passive microwave circuits, reconfigurable RF components, and CP microwave antennas. She is currently a technical reviewer for IEEE TRANSACTIONS ON INDUSTRIAL ELECTRONICS, *Electronics Letters*, and *International Journal of RF and Microwave Computer-Aided Engineering*. She was the recipient of the Best Doctor's Dissertation Award of Liaoning Province in 2017.

SHAOJUN FANG received the Ph.D. degree in communication and information systems from Dalian Maritime University (DMU), Dalian, China, in 2001. Since 1982, he has been with DMU, where he is currently the Head Professor with the School of Information Science and Technology. He has authored or coauthored four books and more than 100 journal and conference papers. His current research interests include passive RF components and antennas. He was the recipient of the Best Doctor's Dissertation Award of Liaoning Province in 2002 and Outstanding Teacher Award of the Ministry of Transport of China.